JETIR.ORG ISSN: 2349-5162 | ESTD Year : 2014 | Monthly Issue
JOURNAL OF EMERGING TECHNOLOGIES AND INNOVATIVE RESEARCH (JETIR)
An International Scholarly Open Access, Peer-reviewed, Refereed Journal

A MECHANISTIC STUDYOF THE OXIDATIVE DECARBOXYLATIONOF PHENYLSULFINYLACETIC ACIDS BY HYDROGEN PEROXIDE CATALYZEDBY OXOVANADIUM(IV)-SALOPHEN COMPLEXES IN THE PRESENCE OF BASES-A NON LINEAR HAMMETT AND LINEAR YUKAWA TSUNO CORRELATION

[1*]R. Jeevi Esther Rathnakumari, [2]C. Kavitha ,[3]V. Vetriselvi [4]P. Subramaniam,[5]J. Janet Sylvia Jaba Rose
[1*]Head &Associate Professor,[2] Head &Assistant Professor
[1]Department of Chemistry, Nazareth Margoschis College, Nazareth 628 617, Tamil Nadu, India
[2]Department of Chemistry, Aditanar College of Arts and Science, Tiruchendur 628202, Tamil Nadu, India

ABSTRACT

The oxovanadium(IV)-salophen catalysed oxidative decarboxylation of phenylsulfinylacetic acids by H_2O_2has been studied spectrophotometricallyin 100% acetonitrile medium under the influence of nitrogen bases like pyridine (Py), imidazole (ImH) and 1-methylimidazole (MeIm).Kineticresults reveal that the reaction rate is highly sensitiveto the nature of baseand strongly retarded by the nitrogen bases.The hydroperoxo species formation and an electrophilic attack of sulfur atom of PSAA on the nucleophilic peroxo oxygen of the vanadium complex is proposed as the mechanistic pathway of the reaction. The linear Yukawa-Tsuno plot correlates that the ground state stabilization of PSAAs through resonance interaction is the cause for the observed non linearity in the Hammett plot.

Keywords: oxovanadium(IV)-salophen, phenylsulfinylacetic acid, non-linear Hammett, oxidative decarboxylation, nitrogen base
***Abbreviations*:** PSAA, phenylsulfinylacetic acid; EWG, electron withdrawing group; EDG, electron donating group; Py, pyridine; ImH, imidazole; MeIm, 1-methylimidazole.

1. Introduction

Vanadyl compounds with different coordination modes have been designed and synthesized for the clinical use (Sakurai et al. 2002 & Liboiron et al. 2005). Vanadium species have been extensively studied for energy conversion in photovoltaic solar cells and fuel cells; and in biological systems owing to their multivalent oxidation states,excellent interactions with molecules or ions and superior catalytic properties (Liu et al. 2017). Oxovanadium catalyzed reactions constitute a vital and powerful role, not only in chemistry but also in biomedical and environmental sciences (Pessoa et al.2019). Heterogeneous catalyst, Mo_3VOx is utilized for the conversion of various biomasses (Bagheri et al. 2017). Besides, several novel photo catalysts have been used for hydrogen evolution and environmental remediation through photocatalytic degradation of hazardous organic pollutants (Karthik et al 2022, Kannan et al. 2021, Kumar et al. 2021 and Hodala et al. 2021). The structural similarities of the salen/salophen vanadium complexes with metalloproteins and enzymes are responsible for their broad range of catalytic applications for a wide range of transformations (McCaffrey et al. 2021, Kargar et al. 2021 & Adam et al. 2021).

Oxidative decarboxylation takes place in the mitochondrial membrane in conjunction with electron transport and oxidative phosphorylation provides the basis of human cell respiration. Anti-inflammatory drugs such as indomethacin and ibuprofen are decarboxylated during metabolism by cytochrome p-450 in vivo and the carbon dioxide released was found to reduce pain. In the present oxidative decarboxylationstudy, phenylsulfinylacetic acid (PSAA), a sulfoxide containing chelating agent is oxidized and decarboxylated to methyl phenyl sulfone. The chemistry of sulfones has been explored due to their antimicrobial (Dixit et al. 2008),

anticancer, anti-HIV (Meadows et al. 2007), antimalarial (Lee et al. 2009)] and anti-inflammatory therapeutic activities. Hence the oxidation of organic sulfur compounds has been the subject of interest in recent years.

Nitrogen bases like pyridine (Py), imidazole (Im) and their derivatives exhibit various types of biological activities *viz.*, antimicrobial, analgesics, anticancer, antidiabetic etc. Several investigations on sulfoxidation reactions involving different mechanisms; namely electrophilic attack of a sulfur atom on the nucleophilic peroxo oxygen atom (Subramaniam et al. 2016), S_N2 type oxygen transfer (Subramaniam & Thamil Selvi, 2013, 2014, 2015 & 2016), direct oxygen transfer (Kavitha, & Subramaniam 2020, Subramaniam et al. 2014 and 2016) and single electron transfer (Subramaniam et al. 2016, Subramaniam, & Shanmugasundari 2017 & Balakumar et al. 2010) have been reported. This paper reveals the mechanistic study of the oxidative decarboxylation of substituted PSAAs by H_2O_2 catalyzed by oxovanadium(IV)-salophen complexes (**I-IV**) in the presence of bases. The overall reaction scheme is represented in Scheme 1.

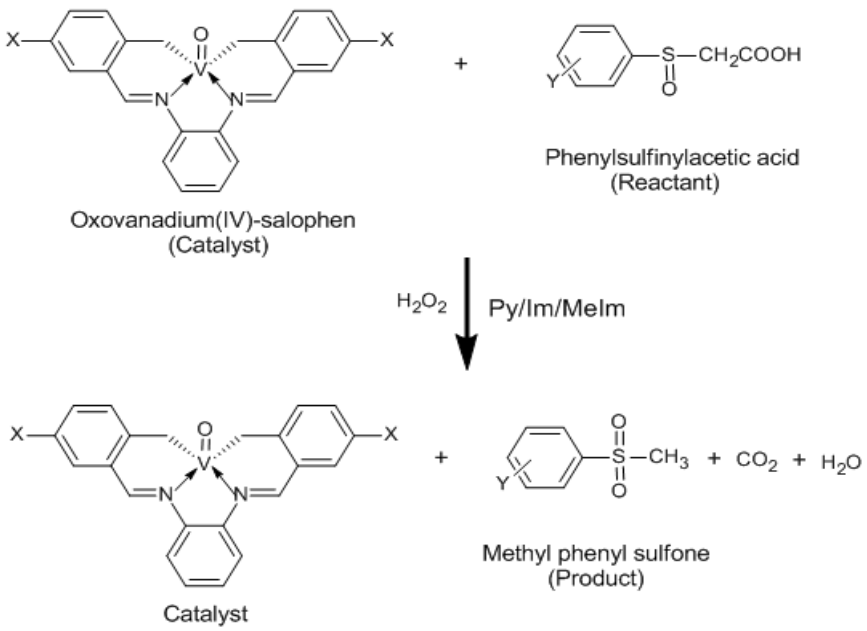

Scheme 1: Complex : X = H (**I**); -OCH_3 (**II**); -CH_3 (**III**); -Cl (**IV**).

PSAA :Y = H; *p*-Cl; *m*-Cl; *p*-F ; *p*-Br ; *p*-Me; *p*-OEt; *p*-OMe.

2. Experimental

2.1. Materials and methods

Salicylaldehyde, 5-methyl, 5-methoxy and 5-chloro salicylaldehydes (Alfa Aeser, 99%), 1,2-benzenediamine (AR Merck, >98%), $VOSO_4.5H_2O$ (Sigma-Aldrich, 97%), methanol and ethanol (SD fine, 99.9%) were purchased and used as such. H_2O_2 (GR, Merck, 30%) and acetonitrile (HPLC grade, Merck, 99.9%) were used as received. The nitrogenous bases (N-bases) used were pyridine (Py) (SD fine, 100%), imidazole (ImH) (AR Merck >99%) and 1-methyl imidazole (MeIm) (Sigma-Aldrich, 99%).

A double beam BL 222 Elico UV–vis bio spectrophotometer with an inbuilt thermostat was employed to record the absorption spectra of oxovanadium(IV)-salophen complexes. LC-MS was performed on a HPLC coupled Agilent ion trap mass spectrometer. Mass spectrometry was done using APCI (+) ionization technique. GC-MS data were acquired using Thermo GC-Trace ultra Ver: 5.0, Thermo MS DSQ II mass spectrometer. Infrared spectrum of the product was recorded using KBr pellet on a JASCO FT/IR-410 spectrophotometer. The elemental analysis (carbon, hydrogen, nitrogen and sulfur) of the materials was obtained from Elementar CHNS Analyser, Model Vario Micro cube.

2.2. Preparation of phenylsulfinylacetic acids

Phenylsulfinylacetic acid and its meta- and para-substituted acids were prepared from the corresponding phenylmercaptoacetic acids by controlled oxidation with an equimolar amount of hydrogen peroxide as reported in the previous paper (Subramaniam et al. 2016) The purity of the PSAAs was checked using their melting points and the elemental analysis done were found to agree with the literature values. The purity of PSAAs were also confirmed by LC-MS analysis.

2.3. Synthesis of the oxovanadium(IV)-salophen complexes

The synthesis of the oxovanadium(IV)-salophen complexes was accomplished by following the literature procedure as mentioned earlier (Subramaniam et al. 2016). All the four oxovanadium(IV)-salophen complexes synthesized were characterized by UV-vis, FT-IR, mass spectral techniques and elemental analysis.

2.4. Kinetic studies

The kinetic study for the reaction of PSAA and substituted PSAAs with H_2O_2 and oxovanadium(IV)-salophen complexes in the presence of nitrogen bases was carried out in 100% acetonitrile medium under pseudo first-order conditions with excess of PSAA

concentration over the oxidant as well as complex concentrations. The progress of the reaction was followed spectrophotometrically by monitoring the decrease in absorbance of the salophen complexes at an appropriate wavelength using a double beam BL 222 Elico UV-vis spectrophotometer. The absorption peaks that were followed for four complexes are 396 nm, ε = 17700 M^{-1} cm^{-1}**(I)**; 436 nm, ε = 10200 M^{-1} cm^{-1}**(II)**; 412 nm, ε = 17100 M^{-1} cm^{-1}**(III)** and 407 nm, ε = 10800 M^{-1} cm^{-1}**(IV)**. Temperature was maintained constant at 30°C. The kinetics of the reaction studied for different variations of the reactants, oxovanadium(IV)-salophen, PSAA and H_2O_2 at various initial concentrations keeping the other reaction conditions as constant has been reported in the earlier paper (Jeevi Esther Rathnakumari et al 2023).

2.5. Product analysis

The characterization of the product was done in a procedure similar to the oxidative decarboxylation of PSAA in the absence of nitrogen bases (Subramaniam et al. 2016). Formation of methyl phenyl sulfone was identified as the only product of the reaction by FT-IR and GC-MS.

3. Results

3.1. Absorption Spectral studies

Oxovanadium(IV) salophen complex (**I**) has an absorption maximum at 396 nm, which arises due to ligand to metal charge transfer transition (LMCT). It is observed that addition of H_2O_2 at a higher concentration to the complex shows an initial increase in the intensity of a new broad absorption peak around 610 nm after certain time interval followed by decrease in absorbance during the course of time, as observed in the absence of nitrogen bases (Subramaniam et al. 2016). This observation clearly indicates the formation of a new vanadium intermediate species in the reaction mixture.

Another observation noted in the kinetic studies with complexes (**I-IV**) in the presence of nitrogen bases is an initial well defined induction period for a definite period of time followed by a gradual decrease in absorbance (Subramaniam et al. 2016). The induction period and initial time taken for the decrease in OD are found to decrease with an increase in temperature (Fig. 1) and concentration of the substrate and hydrogen peroxide. The decrease in induction period observed with temperature in the reaction may be due to the easy formation of the active hydroperoxo vanadium(V) species at high temperature.

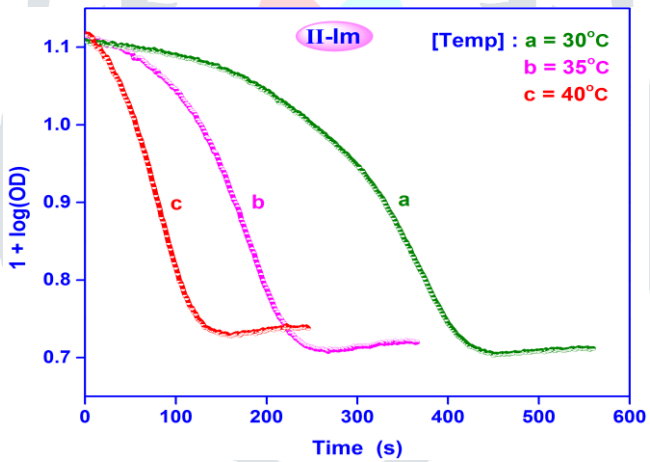

Fig. 1. Pseudo first-order plots at three different temperatures.
[PSAA] = 7.0 × 10^{-2} M; [H_2O_2] = 7.0 × 10^{-3} M; [**II**] = 5.0 × 10^{-5} M; [Im] = 5.0 × 10^{-4} M.

3.2. Effect of PSAA, Hydrogen peroxide and Oxovanadium(IV)-Salophen complex

The reaction is found to exhibit first-order dependence on PSAA for all the four oxovanadium(IV)- salophen complexes in the presence of nitrogen bases.The first-order dependence of rate on H_2O_2 is evidenced from the linear portion observed inthe plot of log(OD) *vs*. time after a period of induction time. Beyond a particular concentrationof H_2O_2, the reaction rate begins to decreaseforall the complexes(**I-IV**).To study the importance of the electronic effect of the substituents, the reactivity of four salophen complexes was compared.The order of reactivity observed among the four oxovanadium(IV)-salophen complexes in the presence of different N-bases is **II** > **III** > **I** > **IV**.

3.3. Influence of Nitrogen bases

To evaluate the effect of nitrogen bases on the reaction rate, the reactions of PSAA and H_2O_2 with complexes **I-IV** were carried out in the presence of nitrogen bases *viz*., Py, Im and MeIm at different concentrations . Kinetic results reveal that the reaction rate is highly sensitive to the nature ofbase and is strongly retarded by all the three nitrogen bases (Jeevi Esther Rathnakumari et al. 2023).

3.4. Effect of substituents and linear free energy relationship

In analyse the nature of transition state and the extent of charge transfer, several *para*- and *meta*- substituted PSAAs were utilized to carry out the reaction with H_2O_2 in the presence of three oxovanadium(IV)- salophen complexes (**I**, **II** and **IV**) and the bases Py, Im and MeIm (Tables 1 & 2). Kinetic data reveals that EWG in PSAA accelerates the rate of the reaction while the EDG retards the reaction rateand the Hammett equation shows a nonlinear downward curvature with two distinct lines for groups

comprising of electron withdrawing and electron donating substituents converging at the parent compound (Fig. 2) as observed earlier (Subramaniam et al. 2016).

Table 1. Second-order rate constants and thermodynamic parameters for the reactions of PSAAs with complex **I** in the presence of nitrogen bases.

X	$10^2\ k_2(M^{-1}\ s^{-1})$			$\Delta^{\ddagger}H$ (kJ mol^{-1})	$\Delta^{\ddagger}S$ ($JK^{-1}\ mol^{-1}$)
	25°C	30°C	35°C		
			Py		
p-Cl	12.5 ± 0.5	15.3 ± 0.32	22.5 ± 1.1	42.2 ± 2.8	-121 ± 6.5
m-Cl	14.0 ± 0.8	16.9 ± 0.10	25.2 ± 0.62	42.0 ± 2.1	-121 ± 7.9
p-F	10.2 ± 0.56	13.6 ± 0.90	18.2± 0.80	44.2 ± 1.6	-116 ± 8.1
p-Br	12.2 ± 0.6	15.1 ± 0.20	23.4 ± 1.0	46.9 ± 2.2	-106 ± 5.4
H	9.80 ± 0.41	12.6 ± 0.53	15.8 ± 1.2	33.9 ± 2.6	-151 ± 4.9
p-Me	6.76 ± 0.26	8.76 ± 0.44	10.2 ± 0.3	28.9 ± 2.0	-171 ± 5.8
p-OEt	6.17 ± 0.80	7.59 ± 0.62	7.94 ± 0.51	16.8 ± 1.2	-212 ± 9.6
p-OMe	4.90 ± 0.30	5.90 ± 0.09	6.31 ± 0.22	16.6 ± 1.8	-214 ± 10.2
ρ_{EWG}	0.436 ± 0.05	0.333 ± 0.02	0.540 ± 0.03		
r	0.996	0.995	0.961		
ρ_{EDG}	0.691 ± 0.06	0.920 ± 0.03	1.16 ± 0.02		
r	0.991	0.999	0.995		
			Im		
p-Cl	12.5 ± 0.32	14.5 ± 0.15	20.1 ± 0.09	33.6 ± 3.1	-150 ± 8.3
m-Cl	13.8 ± 0.06	16.9 ± 0.41	23.2 ± 0.03	37.0 ± 2.8	-138 ± 10.1
p-F	10.9 ± 0.13	13.3 ± 0.24	17.8 ± 0.19	35.1 ± 3.3	-146 ± 9.9
p-Br	12.6 ± 0.41	15.0 ± 0.32	20.9 ± 0.28	36.1 ± 4.2	-142 ± 2.9
H	9.30 ± 0.18	11.6 ± 0.09	14.8 ± 0.05	33.0 ± 2.1	-154 ± 7.2
p-Me	5.65 ± 0.02	6.92 ± 0.06	9.22 ± 0.10	34.7 ± 1.8	-152 ± 8.7
p-OEt	4.09 ± 0.05	5.04 ± 0.02	6.31 ± 0.08	30.4 ± 1.2	-169 ± 9.2
p-OMe	2.18 ± 0.03	2.88 ± 0.04	4.20 ± 0.07	46.6 ± 2.6	-121 ± 3.0
ρ_{EWG}	0.429 ± 0.01	0.398 ± 0.02	0.474 ± 0.06		
r	0.967	0.975	0.970		
ρ_{EDG}	1.45 ± 0.04	1.48 ± 0.02	1.48 ± 0.06		
r	0.994	0.995	0.985		
			MeIm		
p-Cl	10.1 ± 0.13	13.2 ± 0.11	20.4 ± 0.18	50.5 ± 2.5	-95.0 ± 4.1
m-Cl	10.5 ± 0.21	13.6 ± 0.13	22.6 ± 0.16	56.2 ± 3.2	-75.1 ± 3.9
p-F	8.34 ± 0.08	10.6 ± 0.03	15.9 ± 0.10	46.3 ± 2.1	-110 ± 8.8
p-Br	10.9 ± 0.12	12.9 ± 0.08	20.2 ± 0.15	44.4 ± 3.0	-115 ± 1.3
H	7.98 ± 0.04	9.68 ± 0.02	12.3 ± 0.11	30.4 ± 2.2	-164 ± 6.2
p-Me	3.00 ± 0.01	4.54 ± 0.03	6.50 ± 0.08	56.4 ± 3.8	-84.8 ± 5.4
p-OEt	2.14 ± 0.06	2.58 ± 0.02	3.97 ± 0.04	44.5 ± 3.1	-128 ± 7.3
p-OMe	0.980 ± 0.02	1.21 ± 0.03	1.82 ± 0.03	44.7 ± 2.8	-134 ± 10.2
ρ_{EWG}	0.341 ± 0.03	0.413 ± 0.01	0.672 ± 0.02		
r	0.968	0.960	0.956		
ρ_{EDG}	2.40 ± 0.11	2.30 ± 0.09	1.97 ± 0.06		
r	0.999	0.988	0.987		

[PSAA] = 5.0×10^{-2} M; [H_2O_2] = 5×10^{-3} M; [Py] = [Im] = [MeIm] = 5×10^{-4} M; [**I**] = 3×10^{-4} M; Temp. = 30 °C; solvent = 100 % CH_3CN.

It is found that the reaction is fairly susceptible to EWGs with small positive ρ values (0.287 to 0.672) while the EDGs exert a higher effect on the reaction rate as indicated by the fairly high positive ρ values (0.691 to 2.40). The positive ρ values indicate the electrophilic behavior of PSAA towards the oxidant in the reaction.

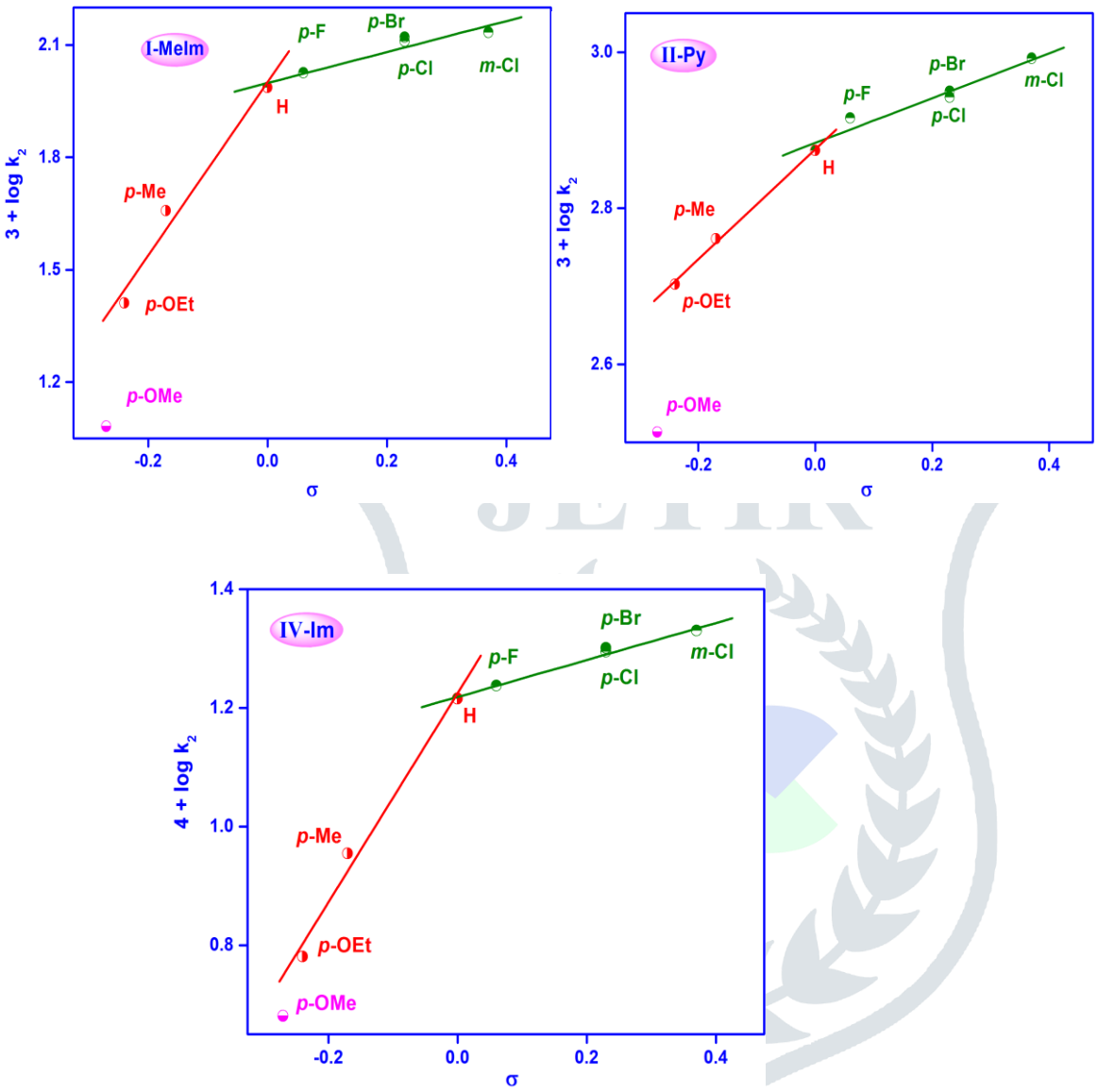

Figure 2. Hammett plots for the reaction between PSAAs and H_2O_2 with complexes. [PSAA] = 5.0×10^{-2} M; [H_2O_2] = 5.0×10^{-3} M; [**I**] = [**II**] = 3.0×10^{-4} M; [**IV**] = 1.0×10^{-4} M; [N-base] = 5.0×10^{-4} M; solvent = 100 % CH_3CN; T = 30 °C.

Table 2 Second-order rate constants for the oxidative decarboxylation of PSAAs by **II** & **IV** in the presence of nitrogen bases.

X	$10^2 k_2$ ($M^{-1}s^{-1}$)					
	II			**IV**		
	Py	Im	MeIm	Py	Im	MeIm
p-Cl	87.5 ± 0.81	63.5 ± 1.1	61.2 ± 0.4	0.199 ± 0.03	0.197 ± 0.02	0.195 ± 0.01
m-Cl	98.2 ± 1.5	68.4 ± 0.08	69.8 ± 0.21	0.224 ± 0.02	0.214 ± 0.01	0.208 ± 0.02
p-F	82.4 ± 2.2	49.0 ± 0.04	53.1 ± 0.06	0.182 ± 0.02	0.173 ± 0.01	0.167 ± 0.01
p-Br	89.1 ± 1.9	61.7 ± 0.05	61.7 ± 0.03	0.209 ± 0.01	0.200 ± 0.02	0.194 ± 0.02
H	74.8 ± 2.3	44.2 ± 0.03	45.6 ± 0.04	0.171 ± 0.01	0.164 ± 0.01	0.161 ± 0.02
p-Me	57.7 ± 1.1	26.2 ± 0.42	28.8 ± 0.21	0.103 ± 0.02	0.090 ± 0.01	0.081 ± 0.01
p-OEt	50.4 ± 0.93	19.1 ± 0.31	22.1 ± 0.19	0.076 ± 0.01	0.060 ± 0.02	0.054 ± 0.02
p-OMe	32.6 ± 0.84	14.4 ± 0.26	16.3 ± 0.10	0.058 ± 0.01	0.048 ± 0.53	0.045 ± 0.02
ρ_{EWG}	0.287 ± 0.02	0.525 ± 0.04	0.465 ± 0.03	0.275 ± 0.01	0.311 ± 0.01	0.312 ± 0.02
r	0.974	0.980	0.980	0.995	0.997	0.991
ρ_{EDG}	0.705 ± 0.11	1.49 ± 0.20	1.28 ± 0.09	1.43 ± 0.02	1.76 ± 0.04	1.93 ± 0.03
r	0.998	0.995	0.996	0.997	0.992	0.997

[PSAA] = 5.0×10^{-2} M; [H_2O_2] = 5×10^{-3} M; [Py] = [Im] = [MeIm] = 5×10^{-4} M; [**II**] = 3×10^{-4} M; [**IV**] = 1×10^{-4} M; Temp. = 30 °C; solvent = 100 % CH_3CN.

3.5. Influence of temperature and thermodynamic parameters

The kinetic study for the reactions of PSAAs and H_2O_2 is carried out with complex **I** at 25, 30 and 35ºC and with complexes (**II-IV**)at 30, 35 and 40ºC in the presence of three N-bases (Table 3). The thermodynamic parameters, $\Delta^{\ddagger}H$ and $\Delta^{\ddagger}S$ evaluated from the slope and intercept of the linear Eyring′s plots (Fig. 3) are shown in Tables 1 and 3. The enthalpy of activation is relatively small in all the four complexes and the entropy of activation is found to be negative. The almost constant activation parameters observed with all the four individual complexes in the presence of three different nitrogen bases confirm that the reaction follows the same mechanism in all cases. The positive $\Delta^{\ddagger}H$ values suggest that the reaction is endothermic in nature. The linear isokinetic relation between $\Delta^{\ddagger}H$ and $\Delta^{\ddagger}S$ (Fig. 4) reveals that all PSAAs follow the same mechanism.

Table 3 Second-order rate constants (k_2) at different temperatures and thermodynamic parameters.

Nitrogen base	10^2k_2 (M^{-1} s^{-1})			$\Delta^{\ddagger}H$ (kJ mol^{-1})	$\Delta^{\ddagger}S$ (JK^{-1} mol^{-1})
	30 ºC	35 ºC	40 ºC		
			II		
Py	59.1 ± 0.51	75.8 ± 2.6	101.4 ± 3.2	40.1 ± 2.6	-117.2 ± 9.2
Im	32.0 ± 1.1	54.6 ± 0.93	66.6 ± 1.3	55.5 ± 3.2	-70.9 ± 4.3
MeIm	47.2 ± 0.62	58.4 ± 0.25	78.6 ± 2.5	37.9 ± 4.5	-126 ± 5.1
			III		
Py	22.4 ± 1.1	28.0 ± 1.0	37.1 ± 0.92	39.3 ± 2.1	-128 ± 10.1
Im	19.7 ± 0.26	26.3 ± 0.81	35.4 ± 1.1	44.4 ± 2.7	-112 ± 9.5
MeIm	15.9 ± 0.36	19.9 ± 0.95	26.6 ± 1.3	40.2 ± 3.6	-128 ± 7.7
			IV[a]		
Py	0.871 ± 0.03	1.57 ± 0.03	2.49 ± 0.11	84.5 ± 5.3	-6.11 ± 1.1
Im	0.594 ± 0.06	0.974 ± 0.01	1.61 ± 0.02	79.8 ± 4.2	-24.3 ± 2.8
MeIm	0.554 ± 0.04	0.868 ± 0.04	1.30 ± 0.07	78.2 ± 3.8	-30.6 ± 3.5

[PSAA] = 7.0×10^{-2} M; [H_2O_2] = 7.0×10^{-3} M; [**II**] = [**III**] = [**IV**] = 5.0×10^{-5} M; [N-base] = 5.0×10^{-4} M; [a][N-base] = 2.5×10^{-4} M; solvent = 100 % CH_3CN.

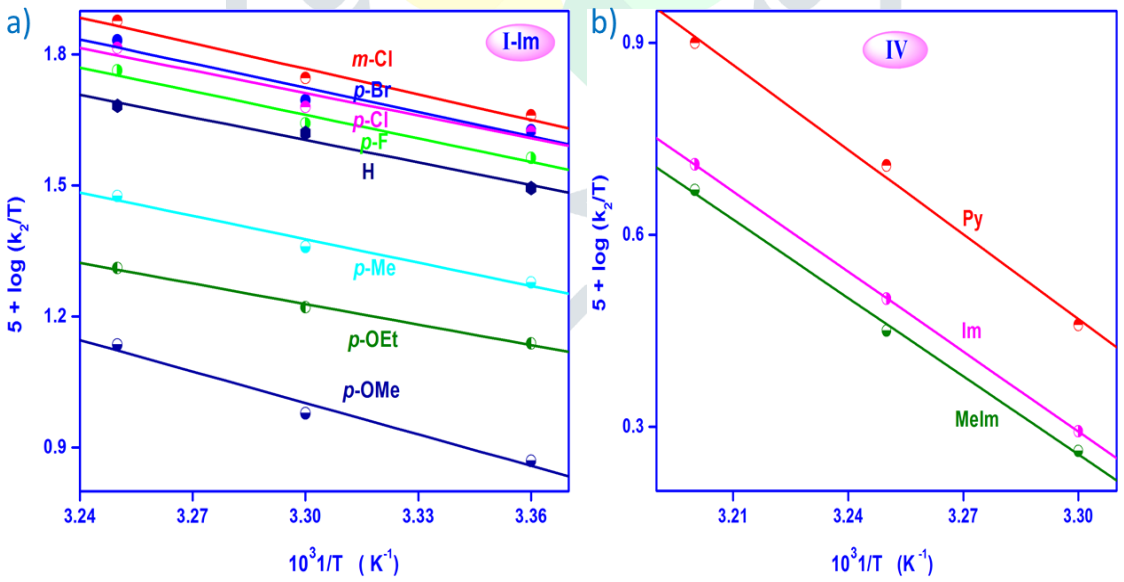

Figure 3. Eyring′s plots for the reactions of PSAAs and H_2O_2 in the presence of complex and N-base; a) General conditions as in Table 1 b) General conditions as in Table 3.

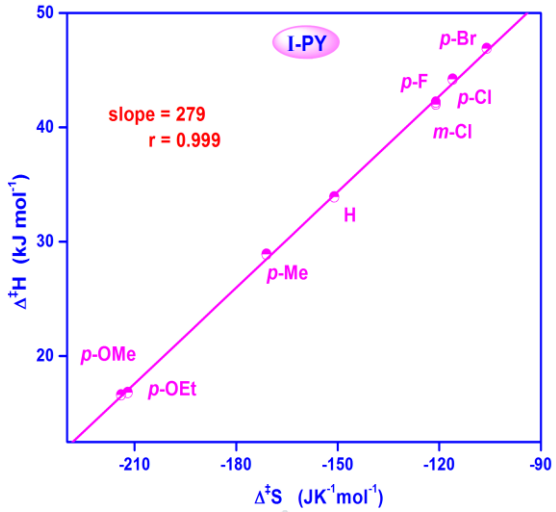

Figure 4. Plot of $\Delta^{\ddagger}H$ *vs.* $\Delta^{\ddagger}S$ for the reactions with **I** in the presence of Pyridine.

4.Discussion

4.1. Mechanism

The hydroperoxo species formed during the reaction is proposed as the mechanistic pathway in the presence of N-base amidst the retarding forces of bases. It is proposed that in the first step, oxovanadium(IV)-salophen complex is oxidized to oxovanadium(V) salophen (**C_1**) .It further reacts with another molecule of hydrogen peroxide in the second step to form the active species, hydroperoxovanadium(V)-salophen (**C_2**). The active species (**C_2**) contains the acidic hydroxyl group and it readily releases a proton and transforms into the intermediate (**C_3**). The proton released from **C_2** polarizes the sulfoxide group of PSAA, rendering sulfur electrophilic in nature. The behaviour of sulfoxide in a reaction can be ascertained from the sign of the ρ value from the Hammett correlation. In the present study from the observed positive ρ values for both electron donating and electron withdrawing groups of PSAA in the Hammett correlation, it is concluded that PSAA behaves as an electrophile.Hence, an electrophilic attack of sulfur atom of PSAA on the peroxo nucleophilic oxygen, leading to the formation of the transition state (**C_4**) in a slow rate determining step is proposed for the reaction. Along with these main steps in the catalytic cycle, two other reactions are also possible in the presence of N-bases.Oxovanadium(IV)-salophen complex combines with the nitrogen base to form the 1:1 oxovanadium(IV)-salophen-nitrogen base adduct (**C_7**) which competes with the formation of active vanadium peroxo species (**C_2**).In addition, the N-base abstracts a proton from the active hydroperoxo oxidizing species (**C_2**) and transforms to a less active cyclic peroxo species (**C_6**) in the catalytic cycle. Based on the above facts, Scheme 2 has been proposed for the oxovanadium(IV)-salophen catalytic oxidation of PSAA by H_2O_2 in the presence of nitrogen bases.

The rate determining step (RDS) proposed is in consistence with the observed substituent effects i.e., increase in rate with EDG in the complex and EWG in PSAA and also decrease in rate with EWG in the complex and EDG in PSAA. The increase in rate with EDG in the complex is attributed to the increase in nucleophilicity of the complex. A similar rate acceleration is observed by Mathavan et al. (2015) in the oxovanadium(IV) salen catalysed H_2O_2 oxidation of tertiary amines. EDG in the phenyl ring of PSAA makes sulfur less electropositive and thus slows down the electrophilic attack of PSAA on the nucleophilic oxygen, whereas the EWG in the phenyl ring of PSAA makes sulfur atom more electropositive and thereby facilitates the electrophilic approach of sulfur towards the nucleophilic peroxo oxygen. The intermediate (**C_4**) then undergoes fast internal oxygen atom transfer leading to the formation of methyl phenyl sulfone with the regeneration of oxovanadium(V) complex.The regeneration of oxovanadium(V)-salophen complex has been confirmed during the product analysis.

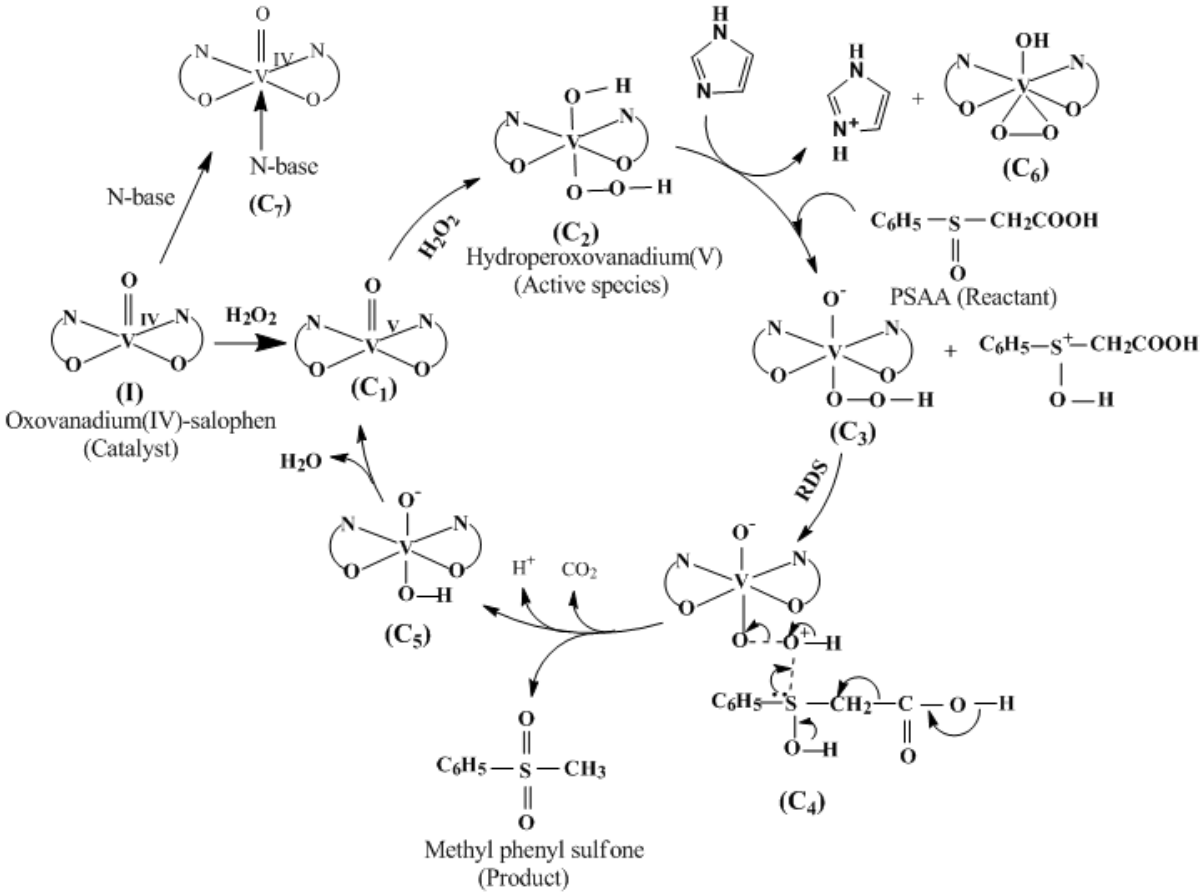

Scheme 2. Mechanistic pathway for the oxovanadium(IV) salophen catalysed oxidation of PSAA by H_2O_2 in the presence of N-bases.

4.2 Role of Nitrogen bases

It has been found that the observed rate retardation with nitrogen base in the present study, is due to the formation of a 1:1 oxovanadium(IV)-salophen-nitrogen base adduct (**C7**) in small amount (Fig. 5) which competes with the formation of active vanadium peroxo species (**C2**).

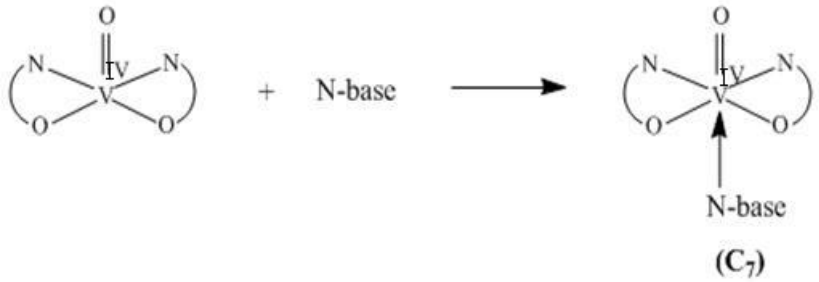

Fig.5. Formation of nitrogen base adduct with complex.

As there is a competition between the peroxo species formation (**C2**) and the 1:1 adduct formation (**C7**) in the reaction mixture, nitrogen bases restrict the free coordination site of oxovanadium(IV)-salophen that would be required for binding of H_2O_2 and for the generation of active species for the reaction to take place. This accounts for the decrease in reaction rate with increase in nitrogen base concentration.

In the present study strong π donating ligands like Im and MeIm have higher retarding effect than less π donating pyridine ligand. This gives a direct evidence that Im and MeIm can form adduct with oxovanadium(IV)-salophen complex more easily than Py which prevents the formation of active hydroperoxo vanadium complex to a greater extent and leads to a higher retardation in reaction rate. The observed order of reactivity among the N-bases is found to be Py > MeIm > Im in complexes **II** and **III** and Py > Im > MeIm in complexes **I** and **IV**. This observed order of reactivity proves that the binding of the N-base with the vanadium atom of the salophen complex is the major cause for rate retardation.

The conversion of more active hydroperoxo oxidizing species (**C2**) to less active cyclic peroxo species (**C6**) in the catalytic cycle, by the abstraction of proton from the active hydroperoxo vanadium species is another possible reason suggested for the retardation of rate with the N-bases. The possibility of existence of the cyclic peroxo species in acetonitrile medium has been proposed by Coletti *et al*. (2012) using theoretical studies. The less active cyclic peroxo intermediate species hinders the oxidation of PSAA by hydroperoxo vanadium(V) species and causes a further retardation in rate. Thus the observed order of reactivity in the presence of nitrogen base unambiguously supports the proposed scheme of mechanism.

4.3. Nonlinear Hammett and linear Yukawa-Tsuno plot

The stabilization of the ground state of PSAA through resonance interaction, on changing the substituents from electron withdrawing to electron releasing is proposed to explain the apparent curvature in the Hammett plots as reported earlier (Subramaniam et al. 2016) The resonance interaction between the electron donating substituent and the thionyl functionality is represented in Figure 6.

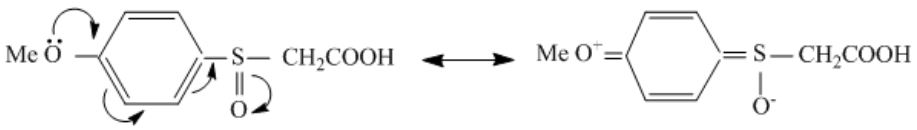

Figure 6. Ground state stabilization of PSAA.

The presence of such resonance structures in electron releasing groups, stabilizes the ground state of PSAA and causes decrease in reactivity (Alenzi et al. 2020). Accordingly, a large ρ value can be expected for EDG when compared with EWG. In fact, the ρ value increases from 0.672 for those with EWG to 2.40 with EDG. Thus, the deviation from Hammett correlation is considered as the evidence for ground state stabilization by EDG.To ascertain the validity of the above argument, the rate data have been treated with the Yukawa-Tsuno equation (Tsuno & Fujio 1999).

$$\log (k_X / k_H) = \rho [\sigma^o + r (\sigma^+ - \sigma^o)]$$

The term $(\sigma^+ - \sigma^o)$ is the resonance substituent constant, while the 'r' value is a parameter characteristic of the extent of resonance contribution. The observed linear Yukawa-Tsuno plots (Fig.7) for the reactions under study and almost unit 'r' values obtained suggest that resonance interaction is relatively significant. The linear Yukawa-Tsuno plots shows that the ground state stabilization of PSAAs through resonance interaction is the cause for the observed non linearity in the Hammett plotand it also confirms a common mechanism for all PSAAs .

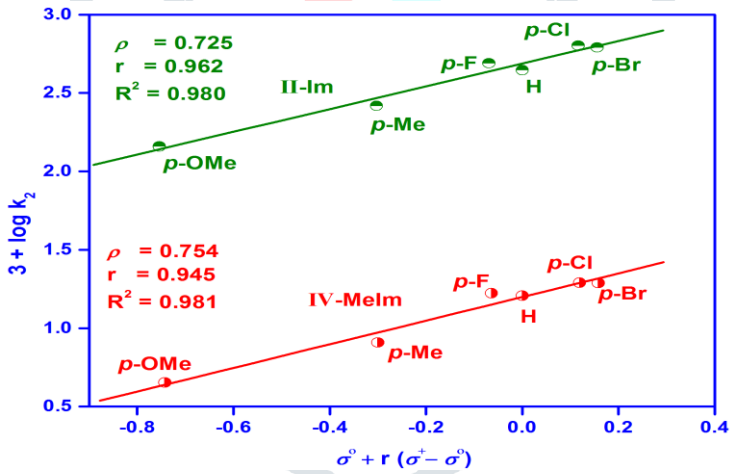

Figure 7. Yukawa-Tsuno plots for the reactions of complexes **II** and **IV** at 30°C in the presence of N-bases.

Conclusion

The mechanism of the oxovanadium(IV)-salophen catalysed oxidative decarboxylation of several phenylsulfinylacetic acids to methylphenyl sulfone by H_2O_2in the presence of N-bases has been investigated. Theresultsshow that nitrogen base forms a 1:1 oxovanadium(IV)-salophen-nitrogen base adductwhich competes with the formation of active vanadium peroxo species. The activehydroperoxo oxidizing species is also converted to less active cyclic peroxo species in the catalytic cycle and thus an impeding effect is observed in the reaction. Vanadium salophen complexes with electron donating substituents on the phenyl groupare found to be more effective catalysts than those with electron withdrawing substituents. A suitable mechanism involving hydroperoxovanadium(V)-salophen as the active oxidizing species has been proposed for the reaction. The linear Yukawa-Tsuno plots and non linear Hammett plots prove the ground state stabilization of PSAAs through resonance interaction. As vanadium catalysts offer competitive reactivity to those of metalloenzymes, additional work has to be done towards the understanding of structure−activity relationships.

Acknowledgements
Financial support from UGC, New Delhi, India in the form of amajor research project (F. No. 39-817/2010(SR)) to PS is gratefullyacknowledged. RJER is thankful to UGC, SERO, Hyderabad (No. F.ETFTNMS181) and Manonmaniam Sundaranar University,Tirunelveli for awarding a fellowship under the FDP programme.The authors are extremely thankful to the Management of AditanarCollege of Arts and Science, Tiruchendur for providing the facilities.

References

1 Adam, M.S.S., Makhlouf, M.M., Ullah, F. and El-Hady, O.M. 2021. Mononucleating nicotinohydazone

complexes with VO^{2+}, Cu^{2+}, and Ni^{2+} ions. Characteristic, catalytic, and biological assessments, Journal of Molecular Liquids 334: 116001.

2 Alenzi, R.A., El Guesmi, N., Shaaban, M.R., Asghar, B.H. and Farghaly, T.A. 2020. Assessing the nucleophilic character of 2-amino-4-arylthiazoles through coupling with 4, 6-dinitrobenzofuroxan: Experimental and theoretical approaches based on structure reactivity relationship, Journal of Saudi Chemical Society, 24(10): 754-764.

3 Bagheri, S. and Muhd Julkapli, N. 2017. Mo_3VO_x catalyst in biomass conversion: A review in structural evolution and reaction pathways, International Journal of Hydrogen Energy, 42(4): 2116-2126.

4 Balakumar, P., Balakumar, S. and Subramaniam, P. 2010. Electron transfer reaction of Iron(III)-bipyridyl Complex with Diphenyl sulfide, Asian Journal of Chemistry, 22: 5723-5729.

5 Balakumar, P., Balakumar, S. and Subramaniam, P. 2012. Application of the Marcus theory to the electron transfer reaction between benzylthioacetic acid and tris(1,10-phenanthroline)iron(III) perchlorate, Reaction Kinetics and Mechanisms Catalysis, 107(2): 253-261.

6 Coletti, A., Galloni, P., Sartorel, A., Conte, V. and Floris, B. 2012. Salophen and salen oxo vanadium complexes as catalysts of sulfides oxidation with H_2O_2: Mechanistic insights, Catalysis Today, 192(1): 44-55.

7 Dixit, Y., Dixit, R., Gautam, N. and Gautam, D.C. 2008. Synthesis of bioactive fluorinated 10H-phenothiazines and their sulfone derivatives, European Journal of Chemistry, 5(S1): 1063-1068.

8 Hodala, J. L., Moon, D.J., Reddy, K. R., Reddy, . C. V., Kumar, T.N , Ahamed, M. I. and Raghu. A.V. 2021. Catalyst design for maximizing C_{5+} yields during Fischer-Tropsch synthesis, Interantional Journal of Hydrogen Energy. 46(4): 3289-3301.

9 Jeevi Esther Rathnakumari, R., Vetriselvi, V., Kavitha, C., Subramaniam, P. and Janet Sylvia Jabarose, J. 2023. Role of nitrogen bases in the oxovanadium (IV)-salophen catalyzed oxidation of phenylsulfinylacetic acids by hydrogen peroxide and the non linear Hammett correlation. The International Journal of Creative Research Thoughts, 11: f343 –f354.

10 Kannan, K., Radhika, D., Reddy, K.R., Raghu, A. V., Sadasivuni, K. K., Palani G. and Gurushankar, K. 2021. Gd^{3+} and Y^{3+} co-doped mixed metal oxide nanohybrids for photocatalytic and antibacterial applications, Nano Express, 2: 010014.

11 Kargar, H., Forootan, P., Fallah-Mehrjardi, M., Behjatmanesh-Ardakani, R., Amiri Rudbari, H., Shahzad Munawar, K., Ashfaq, M. and Nawaz Tahir. M. 2021. Novel oxovanadium and dioxomolybdenum complexes of tridentate ONO-donor Schiff base ligand: Synthesis, characterization, crystal structures, Hirshfeld surface analysis, DFT computational studies and catalytic activity for the selective oxidation of benzylic alcohols, Inorganica Chimica Acta. 523: 120414.

12 Karthik, K.V., Raghu, A.V., Raghava Reddy, K., Ravishankar, R., Sangeeta, M., Shetti, N. P. And Reddy. C.V. 2022. Green synthesis of Cu-doped ZnO nanoparticles and its application for the photocatalytic degradation of hazardous organic pollutants, Chemosphere, 287(2): 132081.

13 Kavitha, C. and Subramaniam, P. 2020. Competitive behavior of nitrogen based axial ligands in the oxovanadium(IV)-salen catalyzed sulfoxidation of phenylmercaptoacetic acid, Polyhedron 189: 114712.

14 Kavitha, C. and Subramaniam, P. 2020. Alteration of electronic effect causes change in rate determining step: Oxovanadium(IV)–salen catalyzed sulfoxidation of phenylmercaptoacetic acids by hydrogen peroxide, Polyhedron 175: 114172.

15 Kumar, S., Reddy, K. R., Reddy, C.V., Shetti, N.P., Sadhu, V., Shankar, M. V., Reddy, V.G., Raghu, A. V., Aminabhavi, T.M. 2021. Metal nitrides and graphitic carbon nitrides as novel photocatalyst for hydrogen production and environmental remediation, Nanostructured Materials for Environmental Applications, 485-519.

16 Lee, P.J., Bhonsle, J.B., Gaona, H.W., Huddler, D.P., Heady, T.N., Kreishman Deitrick, M., Bhattacharjee, A., McCalmont, F.W., Gerena, L., Lopez-Sanchez, M., Roncal, E. N., Hudson, H.T., Johnson, D.J.,Prigge, T.S and Waters C.N. 2009. Targeting the Fatty Acid Biosynthesis Enzyme, β-Ketoacyl−Acyl Carrier Protein Synthase III (PfKASIII), in the Identification of Novel Antimalarial Agents, Journal of Medicinal Chemistry, 52(4): 952-963.

17 Liboiron, Barry D., Thompson, K.H., Hanson, G.R., Lam, E., Aebischer, N. and Orvig, C. 2005. New insights into the interactions of serum proteins with bis (maltolato) oxovanadium (IV): transport and biotransformation of insulin-enhancing vanadium pharmaceuticals. Journal of the American Chemical Society, 127(14): 5104-5115.

18 Liu, M., Su, B., Tang, Y., Jiang, X. and Yu, A. 2017. Recent Advances in Nanostructured Vanadium Oxides and Composites for Energy Conversion. Advanced Energy Materials, 7(23): 1700885.

19 Mathavan, A., Ramdass, A., Ramachandran, M. and Rajagopal, S. 2015. Oxovanadium(IV)-Salen Ion Catalyzed H_2O_2 Oxidation of Tertiary Amines to *N*-Oxides– Critical Role of Acetate Ion as External Axial Ligand, International Journal of Chemical Kinetics, 47(5): 315-326.

20 Mc Caffrey, V.P., Conover, O. Q., Bernard M.A., Yarranton, J.T., Lessnau, N. R.and Hempfling, J.P. 2021. Substituent effects in dioxovanadium(V) schiff-base complexes: Tuning the outcomes of oxidation reactions, Polyhedron 205: 115268.

21 Meadows, D.C., Sanchez, T., Neamati, N., North, T.W. and Gervay-Hague, J. 2007. Ring substituent effects on biological activity of vinyl sulfones as inhibitors of HIV-1,Bioorganic and Medicinal Chemistry, 15(2): 1127-1137.

22 Pessoa, J.C. and Correia, I. 2019. Salan *vs.* salen metal complexes in catalysis and medicinal applications: Virtues and pitfalls, Coordination Chemistry Reviews, 388: 227-247.

23 Sakurai, H., Konjima, Y., Yoshikawa, Y., Kawabe, K. and Yasui, H. 2002. Antidiabetic vanadium (IV) and zinc (II) complexes. Coordination Chemistry Reviews, 226(1-2): 187-198.

24 Subramanian, P., Anbarasan, S., Sugirtha Devi, S., and Ramdass, A. 2016. Modulation of catalytic activity by

ligand oxides in the sulfoxidation of phenylmercaptoacetic acids by oxo(salen)chromium(V) complexes Polyhedron 119: 14-22.

25 Subramaniam, P., Janet Sylvia Jabarose, J. and Jeevi Esther Rathnakumari R. 2016. A paradigm shift in rate determining step from single electron transfer between phenylsulfinylacetic acids and iron(III) polypyridyl complexes to nucleophilic attack of water to the produced sulfoxide radical cation: a non-linear Hammett, Journal of Physical Organic Chemistry, 29(10): 496-504.

26 Subramaniam, P., Jeevi Esther Rathnakumari, R. and Janet Sylvia Jaba Rose, J. 2016. Importance of ground state stabilization in the oxovanadium(IV)-salophen mediated reactions of phenylsulfinylacetic acids by hydrogen peroxide – Non-linear Hammett correlation, Polyhedron 117: 496-503.

27 Subramaniam, P. and Shanmuga Sundari, C. 2017.Oxidative decarboxylation reaction between phenylsulfinylacetic acids and [FeIII(salen)Cl] complex in TX-100 medium, Journal of Chemistry and Chemical Science, 7: 486-494.

28 Subramaniam, P., Sugirtha Devi, S. and Anbarasan, S. 2014. Proximal effect of the nitrogen bases in the oxidative decarboxylation of phenylsulfinylacetic acids by oxo(salen)chromium(V) complexes, Journal of Molecular Catalysis A: Chemical, 390: 159-168.

29 Subramaniam, P., Sugirtha Devi, S. and Anbarasan, S. 2016. Electrophilic and nucleophilic pathways in ligand oxide mediated reactions of phenylsulfinylacetic acids with oxo(salen)chromium(V) complexes, Polyhedron 115: 164-173.

30 Subramaniam, P. and Thamil Selvi, N. 2013. Spectral Evidence for the One-Step Three-Electron Oxidation of Phenylsufinylacetic Acid and Oxalic Acid by Cr(VI), American Journal of Analytical Chemistry, 4(10A): 20-30.

31 Subramaniam, P. and Thamil Selvi, N. 2015. Dynamics of cetyltrimethylammonium bromide-mediated reaction of phenylsulfinylacetic acid with Cr(VI): Treatment of pseudo-phase models, Journal of the Serbian Chemical Society, 80(8); 1019-1034.

32 Subramaniam, P. and Thamil Selvi, N. 2016. Picolinic acid promoted oxidative decarboxylation of phenylsulfinylacetic acid by Cr(VI), Bulletin of Chemical Society Ethiopia, 30(1): 137-146.

33 Subramaniam, P., Thamil Selvi, N. and Sugirtha Devi, S. 2014. Spectral and Mechanistic Investigation of Oxidative Decarboxylation of Phenylsulfinylacetic Acid by Cr(VI), Journal of Korean Chemical Society, 58: 17-24.

34 Tsuno, Y. and Fujio, M. 1999. The yukawa-tsuno relationship in carbocationic systems, Advances in Physical Organic Chemistry, 32: 267-385.